ELSEVIER

Journal of Applied Geophysics 50 (2002) 21–46

JOURNAL OF APPLIED GEOPHYSICS

www.elsevier.com/locate/jappgeo

Nuclear magnetic resonance as a geophysical tool for hydrogeologists

Anatoly Legchenko [a,*], Jean-Michel Baltassat [a], Alain Beauce [a], Jean Bernard [b]

[a] *BRGM, BP 6009, 45060 Orleans Cedex, France*
[b] *IRIS Instruments, BP 6007, 45060 Orleans Cedex, France*

Abstract

The proton Magnetic Resonance Sounding (MRS) is a geophysical technique specially designed for hydrogeological applications. It is based on the principle of Nuclear Magnetic Resonance (NMR) and allows the non-invasive detection of free water in the subsurface. As with many other geophysical methods, MRS is site-dependent. Modeling results show that MRS performance depends on the magnitude of the natural geomagnetic field, the electrical conductivity of rocks, the electromagnetic noise and other factors. For example, the maximum depth of groundwater detection for currently available equipment can vary from 45 to 170 m depending on measurement conditions, although an average depth of investigation is generally considered to be about 100 m. The processing of MRS data can provide the depth, thickness and water content of aquifers. Based on the water content and the relaxation times T_1 and T_2^* provided by MRS, in association with calibration using borehole pumping test data, it is possible to estimate the aquifer's hydrodynamic properties, namely permeability, transmissivity, and specific yield. In this aim, experience gained through NMR logging has been applied to MRS data interpretation and a comparison between the results of borehole pumping tests and those of MRS experiments reveals a good correlation. An example of an MRS survey in Saudi Arabia is presented. The study area is some 1.3 km^2 and underlain by an aquifer composed of fractured diorite. The results of 7 borehole pumping tests and 13 MRS measurements show good agreement. © 2002 Published by Elsevier Science B.V.

Keywords: NMR; PMR; MRS; Surface NMR; SNMR; Magnetic resonance; Near-surface; Groundwater; Geophysics

1. Introduction

The proton Magnetic Resonance Sounding (MRS) method for groundwater investigation was developed in Russia in the early eighties by a team of Russian scientists who then built the first MRS equipment named HYDROSCOPE (Semenov, 1987; Semenov et al., 1987, 1988). The starting point of their research programme was the Varian patent (Varian, 1962), which proposes the use of Nuclear Magnetic Resonance (NMR) for the non-invasive detection of proton-containing liquids (hydrocarbons or water) in the subsurface. The MRS method is used routinely in Russia and has been tested in other countries (Schirov et al., 1991; Goldman et al., 1994; Lieblich et al., 1994; Legchenko et al., 1995, 1997a; Gev et al., 1996). Since 1996, when the MRS equipment NUMIS became commercially available through IRIS Instruments, an interest has developed in the international scientific community to learn more about this method.

* Corresponding author. Tel.: +33-2-38-64-32-37; fax: +33-2-38-64-33-61.
E-mail address: a.legtchenko@exchange.brgm.fr (A. Legchenko).

0926-9851/02/$ - see front matter © 2002 Published by Elsevier Science B.V.
PII: S0926-9851(02)00128-3

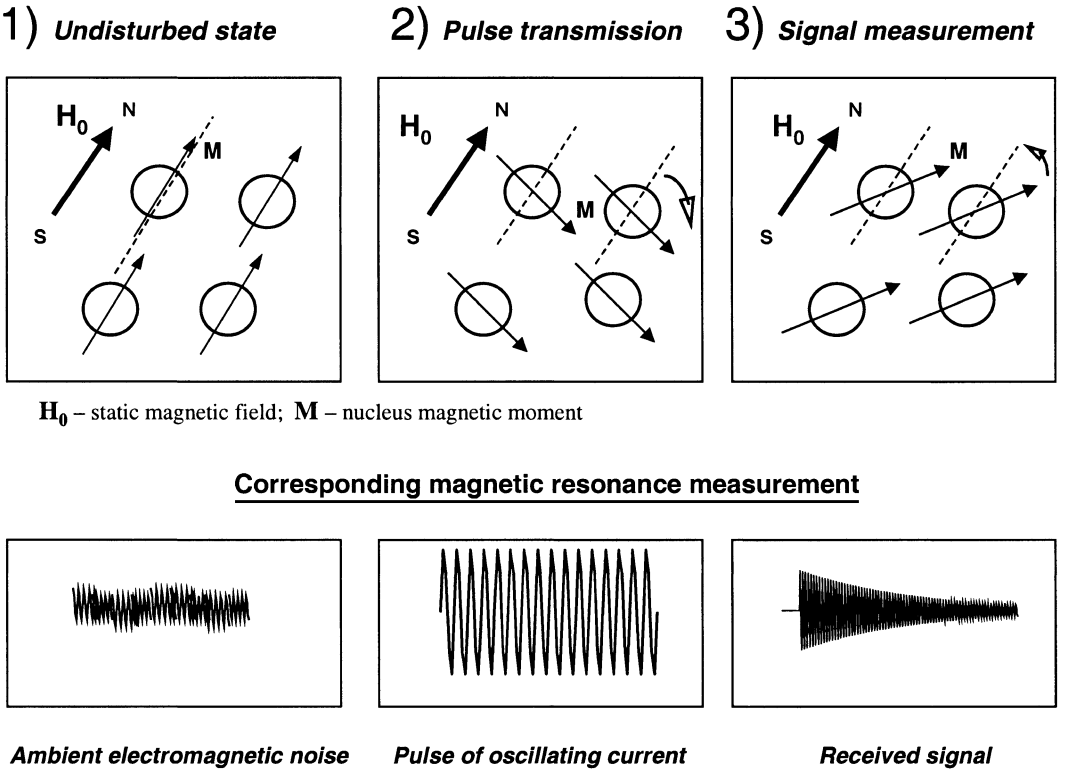

Fig. 1. Typical phases of a magnetic resonance experiment.

The vertical distribution of water content provided by MRS reveals the depth and thickness of aquifers. Recent results show that by combining MRS data with experience gained through NMR logging it is also possible to estimate the effective porosity and permeability of aquifers. Accuracy of the estimation depends on the empirical relationships between the amplitude and relaxation time of the magnetic resonance signal and the hydrodynamic characteristics of the aquifer. Different empirical estimators exist based on laboratory and borehole measurements. However, as permeability is a scale-dependent parameter, and because the MRS provides data averaged over a large volume, the MRS results should be compared with both laboratory measurements and borehole pumping test data.

The basic principles of the MRS method are presented and, based on numerical modeling and field examples, we demonstrate the performance that users can expect from this technique.

2. Nuclear Magnetic Resonance

Nuclear Magnetic Resonance, a phenomenon that can be observed in nuclei possessing a magnetic moment (Slichter, 1990), was discovered by Bloch and Purcell in 1946. The nuclei are generally in

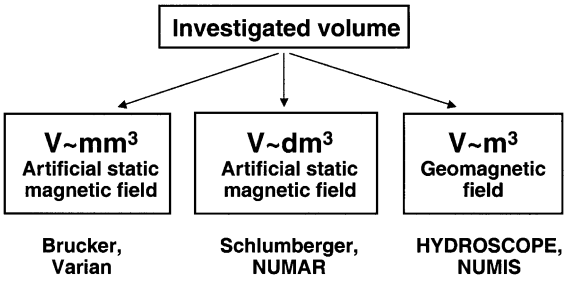

Fig. 2. Classification of NMR equipment by volume of investigated sample.

equilibrium with the environment, and are able to absorb and transmit electromagnetic energy at a specific frequency called the Larmor frequency $f_0 = \gamma H_0/2\pi$. H_0 is the magnitude of the static magnetic field and γ is the gyromagnetic ratio. γ has a specific value for each type of nucleus, and hence the Larmor frequency is a physical property of the nuclei. By selecting the Larmor frequency, one can decide which nuclei will be investigated, thus rendering the NMR method selective.

In the classical model, nuclei are represented as macroscopic magnetic moments M. A typical magnetic resonance experiment consists of three phases (Fig. 1). In the natural undisturbed state (equilibrium), all magnetic moments M are oriented according to the static magnetic field H_0 and nuclei are able to absorb electromagnetic energy at the Larmor frequency. When an external electromagnetic field is applied to the sample, the magnetic moments precess from their equilibrium. When this field is terminated, they return to their initial position and generate a magnetic field, which is also oscillating at the Larmor frequency. This field can be measured and then analysed. For data acquisition, an oscillating current pulse at the Larmor frequency is fed into the transmitting coil. The magnetic resonance response

$$e(t) = E_0 \exp(-t/T_2^*)\cos(2\pi f_0 t + \varphi_0). \quad (1)$$

is recorded at the same frequency after the pulse is terminated. A typical example of data acquisition is presented in the lower part of Fig. 1. Ambient electromagnetic noise is recorded over a few hundreds of milliseconds before the external pulse is transmitted. After an instrument delay known as "dead time", the magnetic resonance signal is measured. The records before and after the pulse are compared to determine whether a magnetic resonance response is detected or not. As noise is independent of the transmitted pulse, a stacking procedure is used to improve the signal-to-noise ratio (S/N).

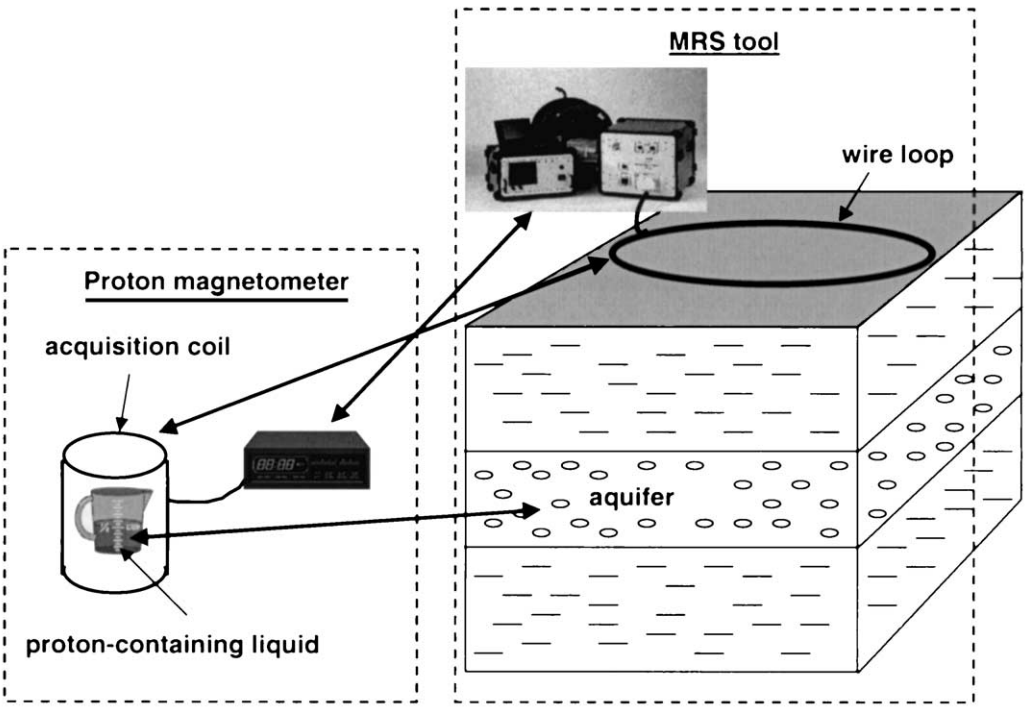

Fig. 3. The MRS tool and a proton magnetometer.

Amplitude of the magnetic resonance response is proportional to the volume of sample investigated and to the square of the static magnetic field $E_0 \sim H_0^2 V$. Thus, the static magnetic field and/or the volume of sample can be increased so as to increase the signal to noise ratio.

Generally, NMR equipment can be classified according to the volume of investigated sample (Fig. 2). Chemical NMR spectrometers and Magnetic Resonance Imaging (MRI) instruments used in medicine, which offer a very high spatial resolution and are commonly used in laboratories, operate on a broad artificial static magnetic field and a small sample volume (mm^3). Much larger sample volumes (a few dm^3) and smaller artificial static magnetic field are used in borehole geophysics (e.g., the Schlumberger and NUMAR tools), whereas surface NMR equipment (such as HYDROSCOPE and NUMIS) operates on the geomagnetic field and sample volumes of a few thousand cubic meters.

3. The proton Magnetic Resonance Sounding method

A comparison between the MRS tool and the well-known proton magnetometer is shown in Fig. 3. The acquisition coil of the MRS tool is larger than that of the magnetometer and forms a circular (or square) wire loop that is laid down on the surface. Subsurface water-saturated layers represent the investigated sample. The natural geomagnetic field is used as the static magnetic field that defines the Larmor frequency for protons (between 800 and 2800 Hz around the world). Since only protons in groundwater can generate a magnetic resonance signal at this frequency (for the first 100–200 m), MRS is in reality a direct method for groundwater detection from the surface.

Three parameters of the magnetic resonance signal (Eq. (1)) are measured after the "dead time" delay τ_{dead}: amplitude E_{0d}; relaxation time T_2^* and phase φ_{0d}. The initial amplitude of the signal E_0 depends on

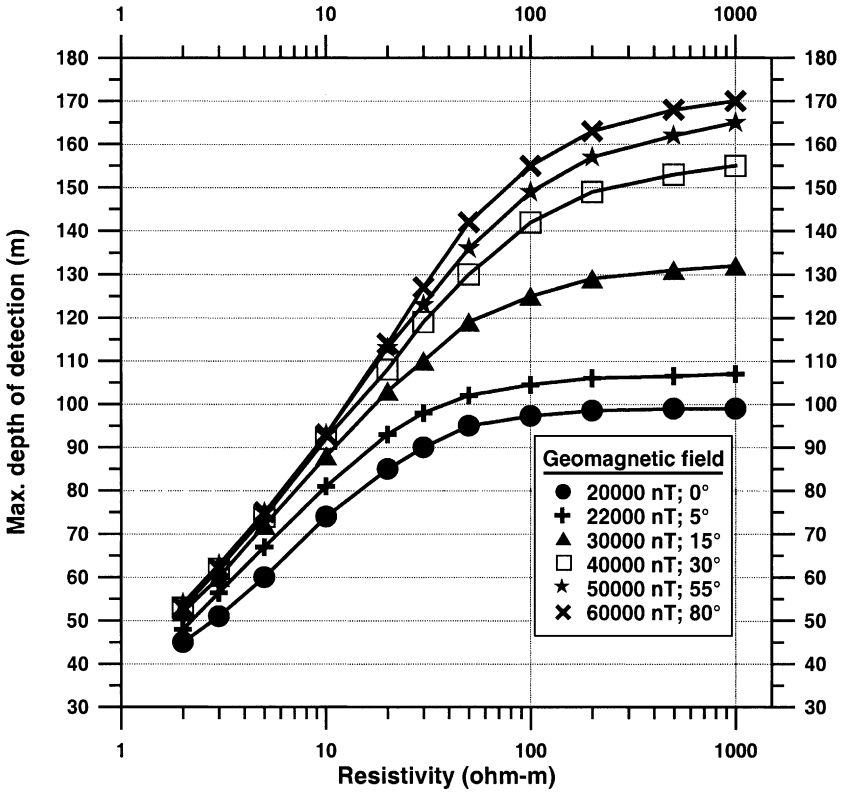

Fig. 4. Maximum depth of detection calculated for a 1-m-thick layer of free water ($w = 100\%$) versus half-space resistivity.

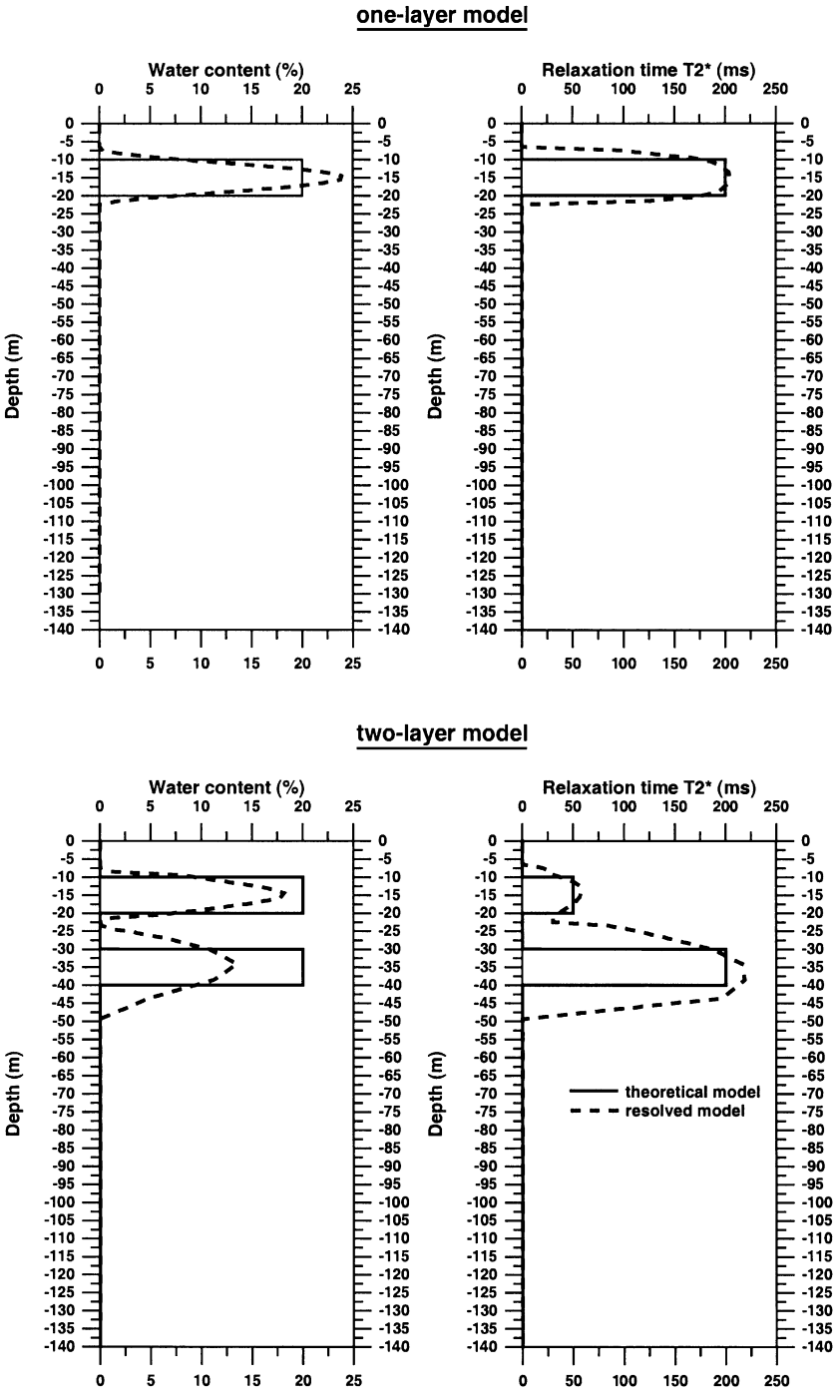

Fig. 5. Examples of resolution of the synthetic models.

the number of protons and hence on the quantity of water. It is obtained by extrapolation using the measured amplitude E_{0d} and the relaxation time T_2^* as

$$E_0 = E_{0d}\exp(\tau_{dead}/T_2^*). \quad (2)$$

The initial amplitude E_0 is a function of the pulse parameter $q = I_0\tau$, where I_0 and τ are respectively the pulse amplitude and duration, and the sounding consists in measuring E_{0d}, T_2^*, and φ_{0d} whilst varying the pulse parameter q.

The phase φ_{0d} correlates with the electrical conductivity of the rocks, but it is not currently used for MRS data interpretation.

3.1. Depth of investigation

The magnetic resonance signal is sensitive to different natural factors, thus making the performance of the method site-dependent. The most common and practically important variations in the magnetic resonance signal are related to the natural geomagnetic field and the electrical conductivity of rocks (Shushakov, 1996; Legchenko et al., 1997b). The electrically conductive subsurface attenuates alternating electromagnetic fields by a factor characterized by the "skin depth" that is proportional to $\sqrt{\rho/f}$, where ρ is the resistivity of the subsurface, and f is the frequency of the electromagnetic field. The Larmor frequency used in MRS is proportional to the geomagnetic field magnitude $f_0 \sim H_0$. Consequently, in areas with a low geomagnetic field (towards the equator) the frequency is lower, and the attenuation caused by the subsurface is less marked than in areas with a high geomagnetic field (towards the poles). However, the magnetic resonance response is proportional to the square of the geomagnetic field $E_0 \sim H_0^2$, which improves the signal-to-noise ratio in areas with a high geomagnetic field, even taking into account the attenuation caused by the subsurface. The inclination of the geomagnetic field also modifies the magnetic resonance signal (Legchenko et al., 1997b). A numerical demonstration of the influence that these natural factors have on the maximum depth of investigation of the MRS method is presented in Fig. 4. The

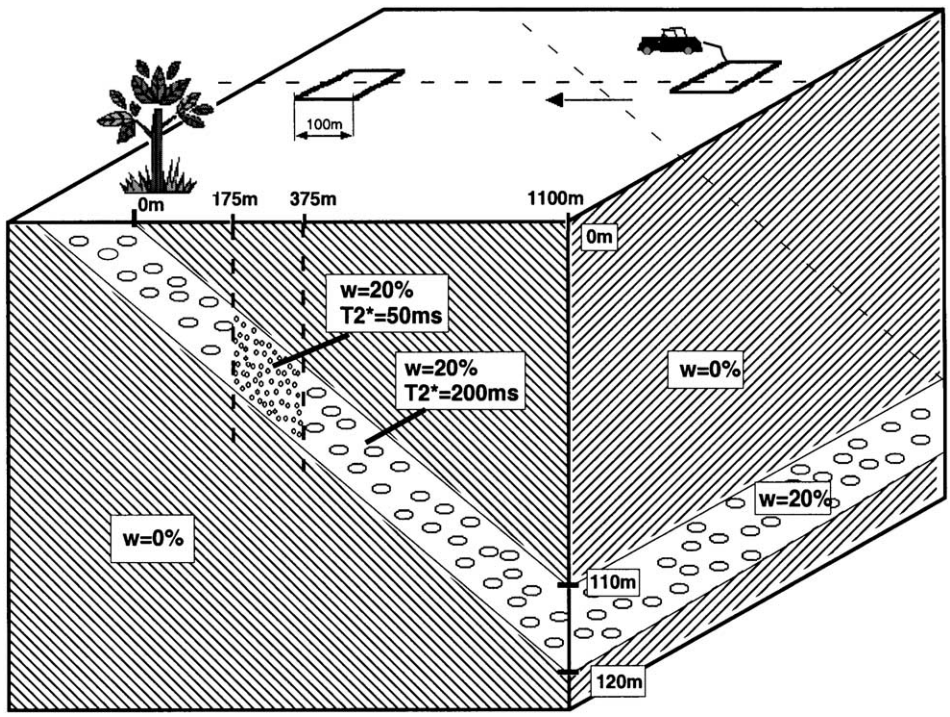

Fig. 6. Definition of the one-layer model.

maximum depth of detection of a 1-m-thick infinite horizontal layer of water (100% water content, and $T_2^* = 1000$ ms) in a noise-free environment is depicted versus half-space resistivity. Calculations were performed for different geomagnetic fields that could correspond to different sites geographically located from poles (large magnitude) to the equator (small magnitude) using the NUMIS^{PLUS} standard configuration, i.e. a 100×100 m square loop, a signal detection threshold of 10 nV, and a maximum pulse of 12,000 A-ms. Magnitude and inclination of the geomagnetic field are seen to be major factors that determine MRS performance when the subsurface is non-conductive. The influence of electrically conductive layers becomes important when their resistivity is less than approximately 50 Ω·m.

3.2. Water content

In the MRS method, the water content in layer i is defined as

$$w_i = E_{0i\_\mathrm{meas}}/E_{0i\_\mathrm{ref}}, \quad (3)$$

where E_{0i_meas} is the measured amplitude of the magnetic resonance signal from a horizontal, infinite,

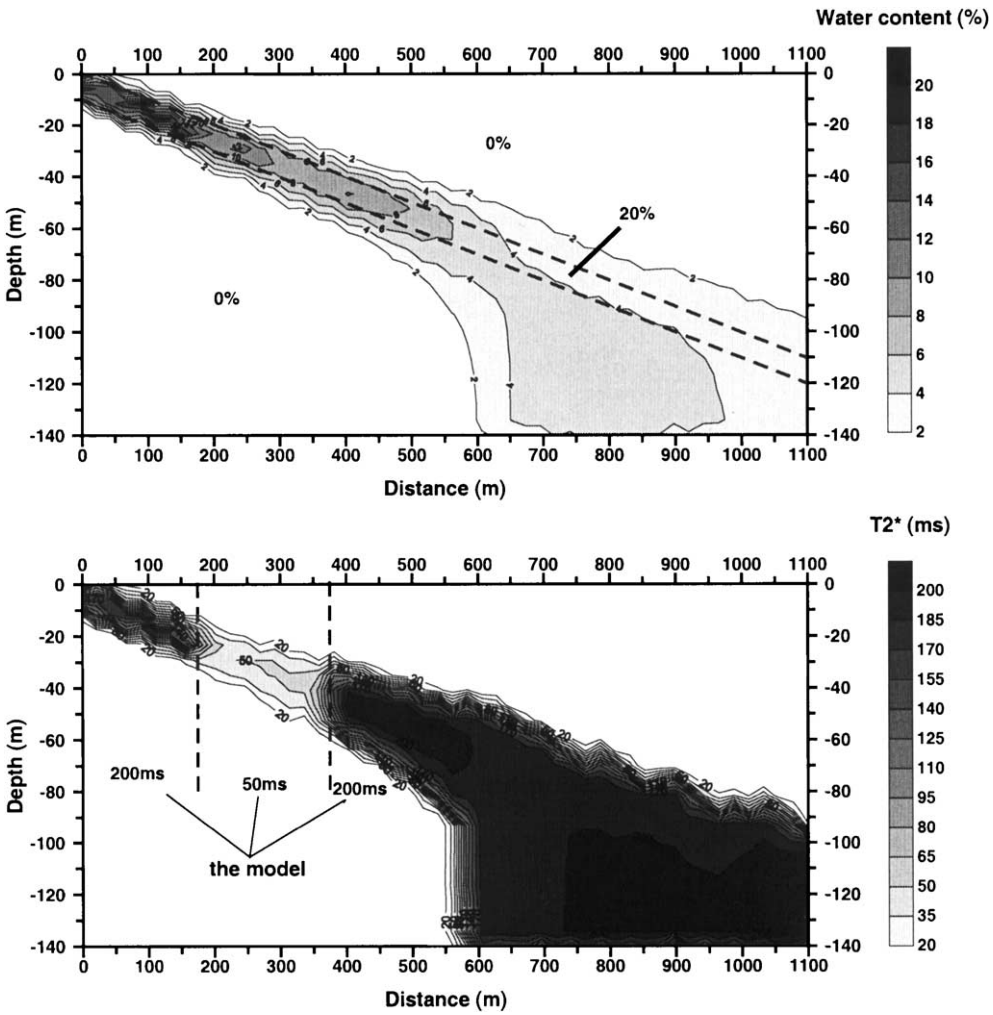

Fig. 7. Resolution of the one-layer model.

water-saturated layer with a thickness Δz_i and at a depth z_i, and E_{0i_ref} is a theoretical signal calculated assuming that the same layer (z_i, Δz_i) is filled with 100% of water. However, this definition does not take into consideration relaxation effects that may make the signal shorter than the MRS equipment is able to detect in certain parts of the investigated volume. For the layer (z_i, Δz_i) with an investigated volume V, let V_W be the part of the layer filled with water, and V_R be the part occupied by rock ($V = V_W + V_R$). The water volume V_W can be divided into two parts, namely water in pores (between grains) known as ''free water'' that can be extracted (V_{free}), and water attached to grains known as ''bound water'' that cannot be extracted (V_{bound}), thus $V_W = V_{free} + V_{bound}$. Because of the small distances involved, interactions between grain surfaces and protons of ''bound water'' mean that the relaxation time of the magnetic resonance signal from ''bound water'' is less than that from ''free water''. Since the very short signals from bound water cannot be measured by currently available equipment, the water content measured by MRS can be defined as the part of the total volume of the subsurface occupied by free water:

$$w = C_W V_{free}/V. \quad (4)$$

As no direct relationship exists between the mobility of water in the aquifer and relaxation time of the magnetic resonance signal used in MRS to discriminate between bound and free water, a calibration constant C_W is needed that establishes an empirical

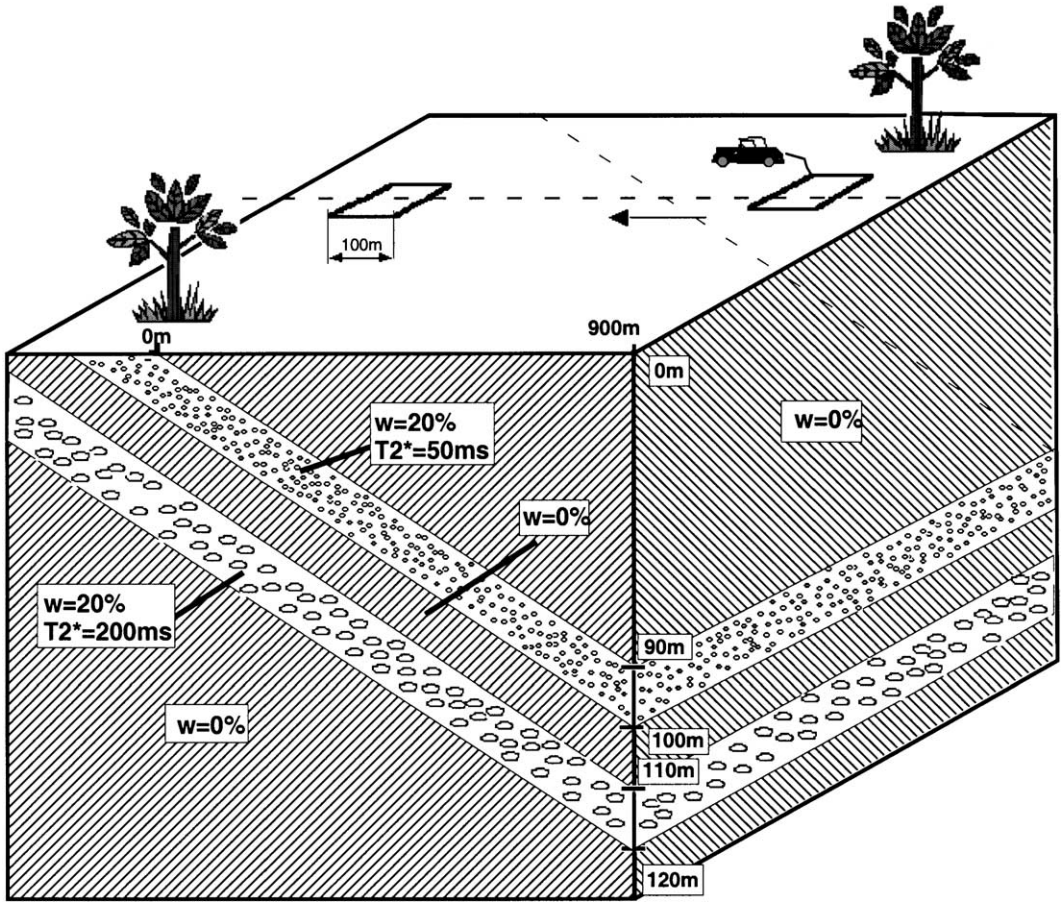

Fig. 8. Definition of the two-layer model.

relationship between these two parameters for different rocks. When calibration is possible, water content can be considered as an estimate of effective porosity, for example, $w = 0\%$ for dry material and $w = 100\%$ for bulk water in a lake.

In order to establish a quantitative correspondence between the water content derived from MRS data and the effective porosity used in hydrogeology a further research is required.

3.3. Vertical resolution

The inversion of MRS data ($E_{0d}(q)$ and $T_2^*(q)$) provides the depth (z), thickness (Δz), water content (w), and relaxation time T_2^* for each water-saturated layer. However, like many other geophysical problems, the MRS inverse problem is ill-posed and therefore the solution is not unique (Legchenko and Shushakov, 1998). We present "smooth inversion" results per-

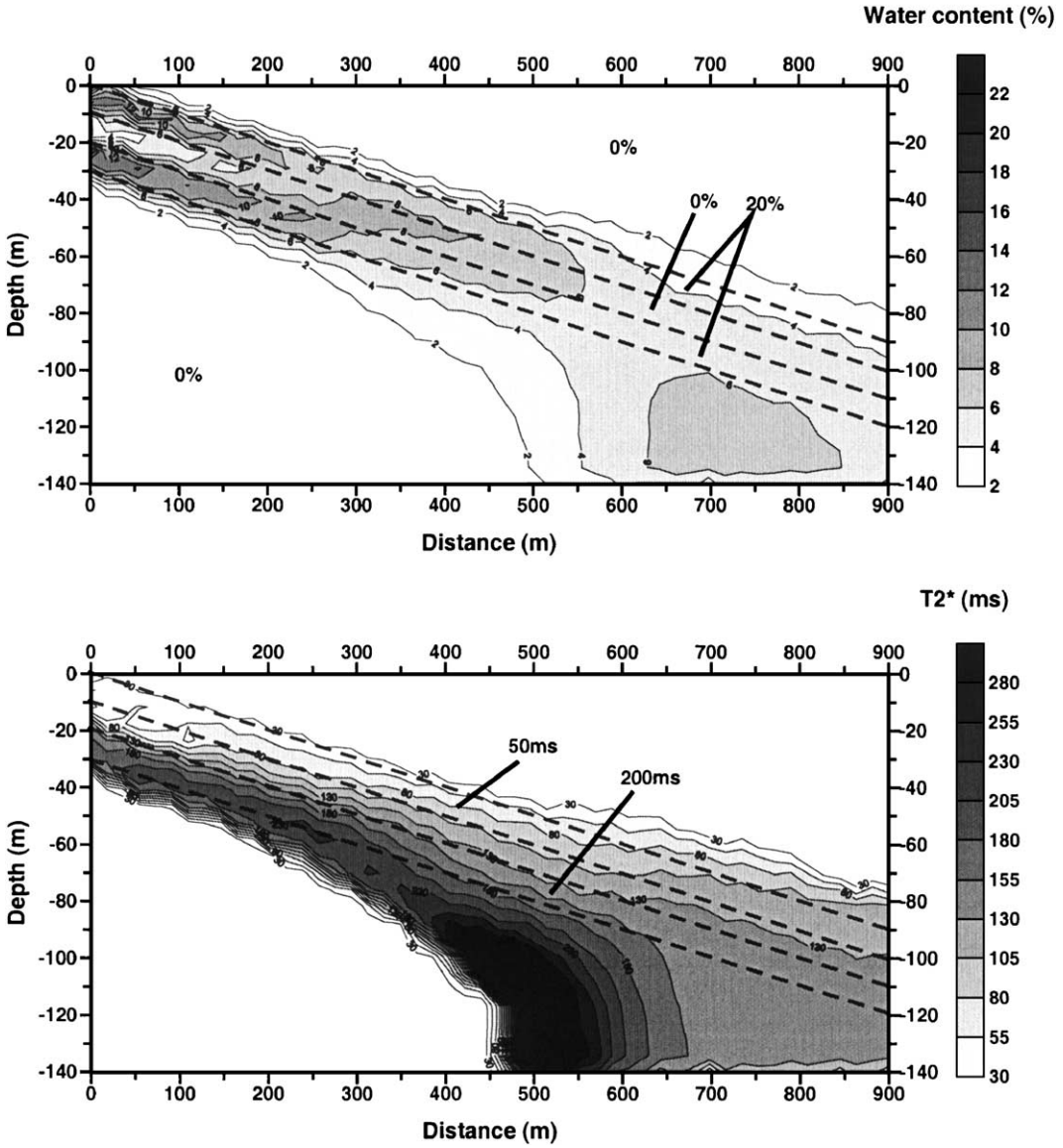

Fig. 9. Resolution of the one-layer model.

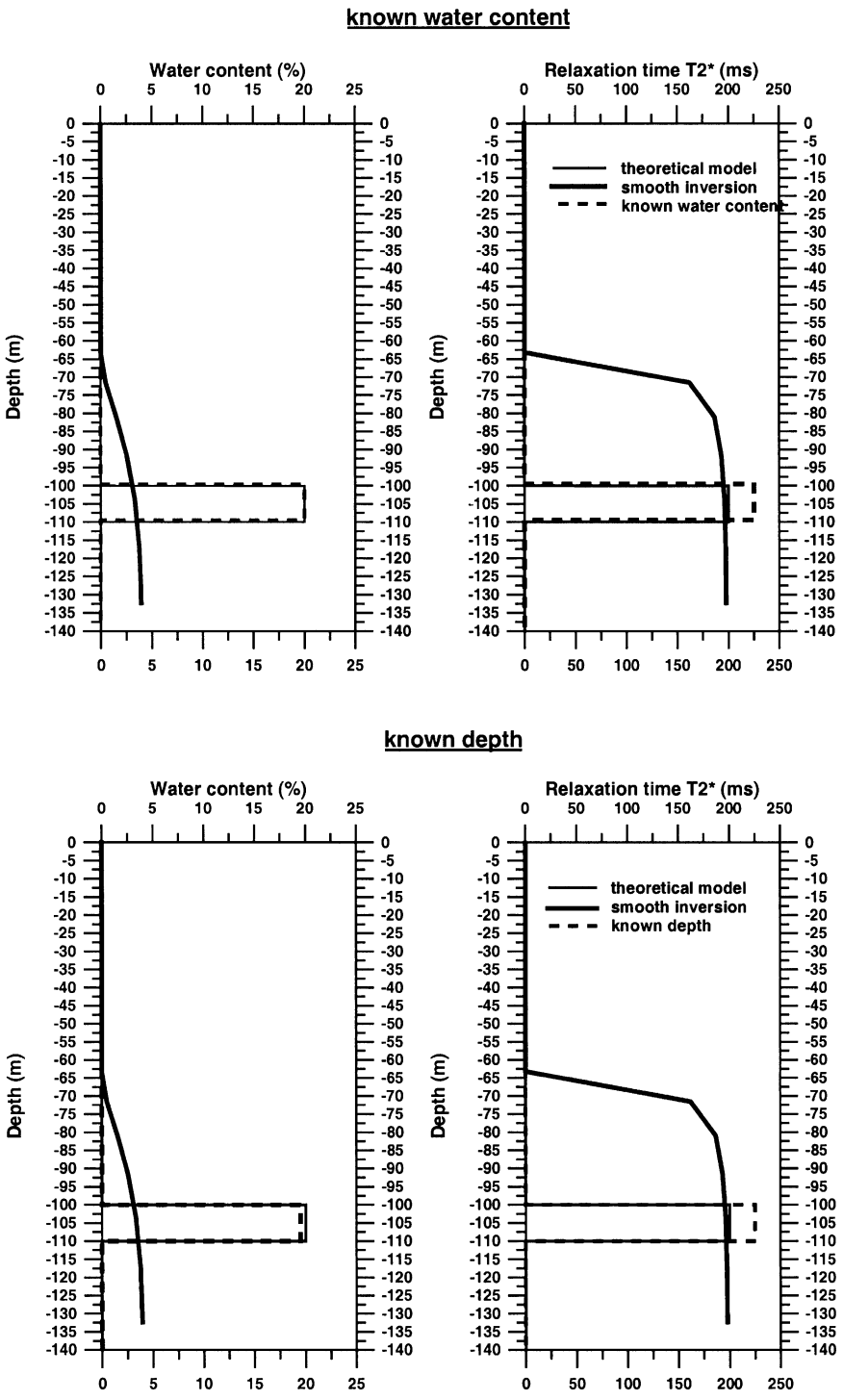

Fig. 10. Examples of resolution of the synthetic one-layer model using known water content and known depth inversions.

formed according to the Tikhonov regularization method, but other methods could equally be used (Guillen and Legchenko, 1997, 1998). Some examples of synthetic data inversion are presented in Fig. 5 where two models are studied:

a one-layer model ($w = 20\%$; $T_2^* = 200$ ms, $z = 10$ m; $\Delta z = 10$ m),

and a two-layer model ($w_1 = 20\%$; $T_{2\_1}^* = 50$ ms, $z_1 = 10$ m; $\Delta z_1 = 10$ m, $w_2 = 20\%$; $T_{2\_2}^* = 200$ ms, $z_2 = 30$ m; $\Delta z_2 = 10$ m).

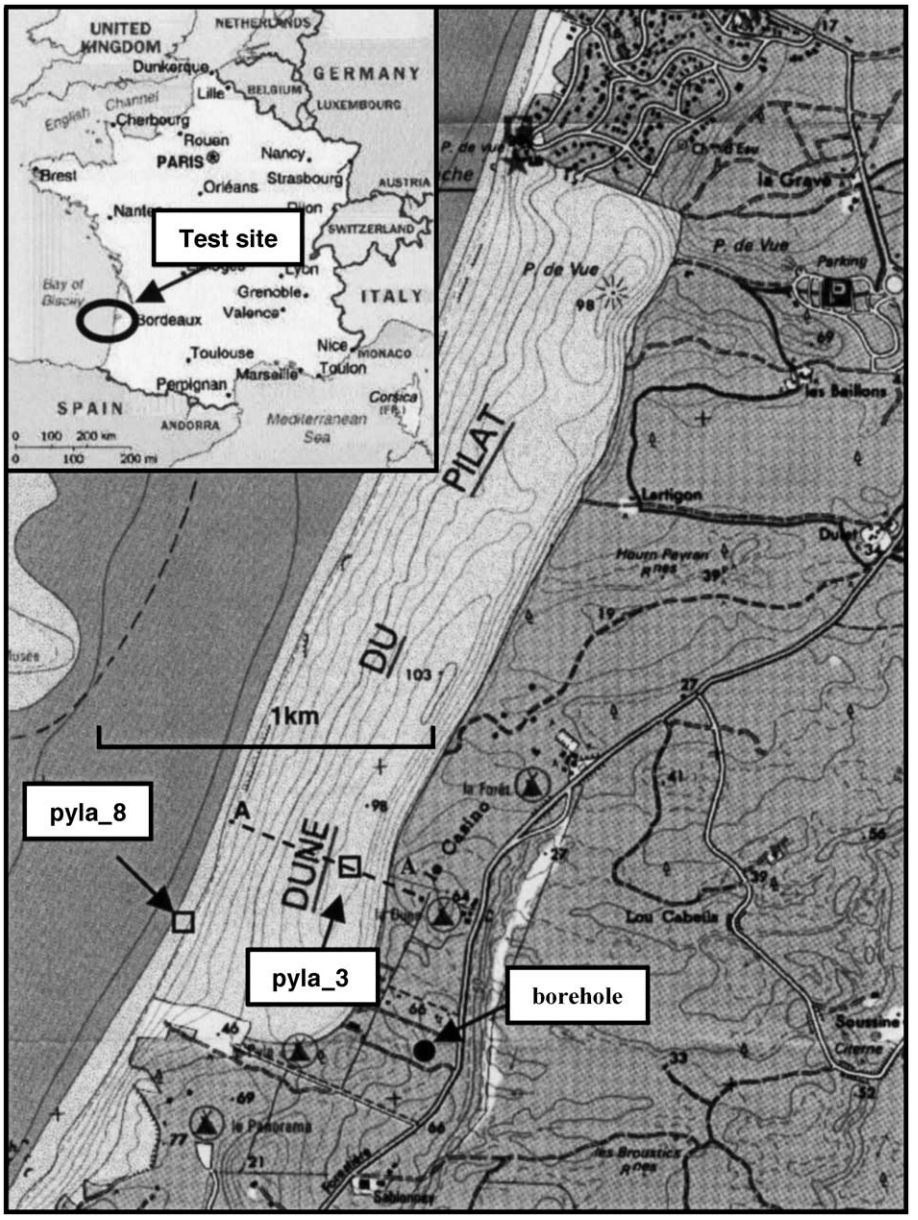

Fig. 11. Map of the Dune du Pilat area showing the location of the MRS test sites.

For modeling purposes, we assume a 100 × 100 m square loop, a 100 Ω·m half space for the subsurface, and a geomagnetic field of 47,000 nT with an inclination of 55°. The theoretical models are depicted using solid lines and the dashed lines represent the inversion results. We can see that the one-layer model is better resolved than the more complicated two-layer model.

Previous studies have shown that resolution of the MRS method decreases with increasing depth. This can be demonstrated by computing MRS signals from an inclined 10-m-thick water-saturated layer that is shown in Fig. 6. We assume that the soundings are performed along a profile running from the deepest to the shallow part of the layer. The relaxation time T_2^* is supposed to be shorter between 175 and 375 m. The results of 1D inversion for water content (w) and relaxation time (T_2^*) are plotted versus distance (Fig. 7); the model is also represented with dashed lines. Resolution is seen to decrease progressively with increasing depth. While the top of the layer (z) is relatively well resolved down to 100 m, the thickness of the layer is resolved down to about 60–70 m, below which neither thickness (Δz) nor water content (w) can be derived from the MRS data. Relaxation time (T_2^*) is well resolved down to 100 m for this one-layer model.

The more complicated two-layer model is depicted in Fig. 8 and the inversion results are presented in Fig. 9. The two layers are resolved individually down to about 40 m, below which they are depicted as a single layer. Relaxation time is resolved down to 70–80 m.

The modeling results show that although the MRS method is able to detect water down to a depth similar to or even greater than the loop size, it is only able to resolve the actual aquifers down to about half this depth.

We have considered MRS resolution for the case where inversion is carried out without any additional knowledge of the subsurface. When such data are available for interpretation, however, the MRS results

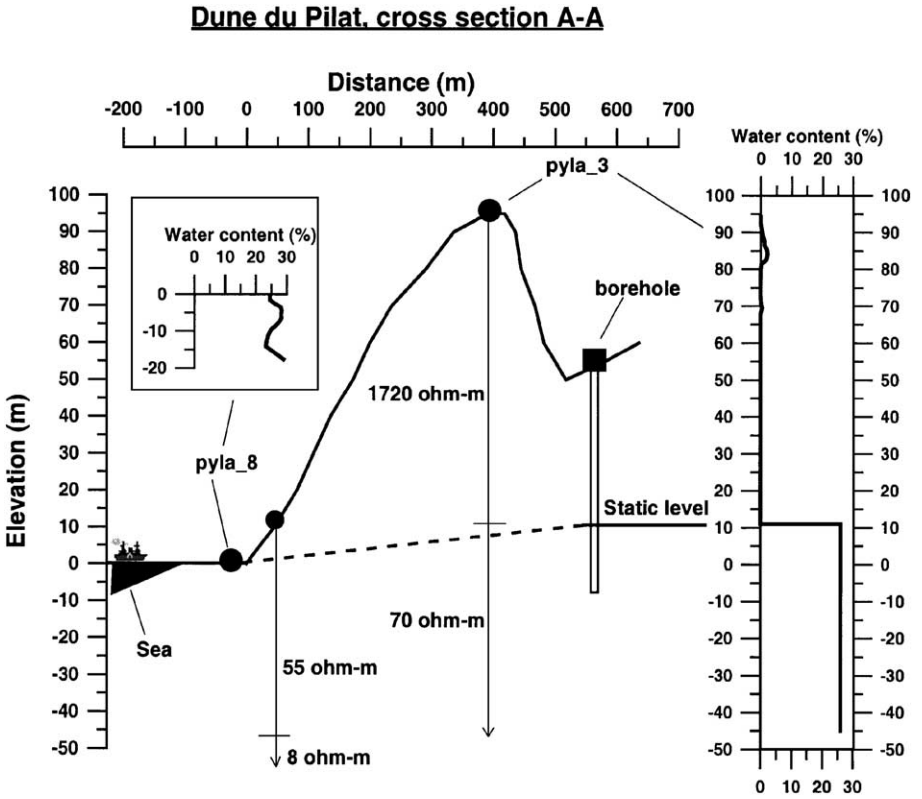

Fig. 12. Dune du Pilat: MRS results.

can be improved. Inversion results for the one-layer model ($w = 20\%$; $T_2^* = 200$ ms, $z = 100$ m; $\Delta z = 10$ m) are presented in Fig. 10. The theoretical model is depicted with a thin solid line, and the smooth inversion results are shown with a thick solid line. When water content ($w = 20\%$) or depth ($z = 100$ m; $\Delta z = 10$ m) is known, then the inversion results can be significantly improved, as shown in Fig. 10 by the dashed lines.

In order to assess the ability of the method to detect aquifers at a depth greater than the loop size, two MRS experiments were performed in the Dune du Pilat area (Fig. 11) that is covered by a large sand dune 2 km long, 500 m wide and 100 m high. The water table is governed by sea level. The results of two TDEM soundings and measurements of the static level in a nearby borehole were also available. The cross-section A–A and the geophysical sounding results are depicted in Fig. 12. The first sounding *pyla_8* was carried out on the beach where the water table is very close to the surface using a 19×19 m square loop. The smooth inversion revealed the water content in the aquifer to be about 26%. The second sounding *pyla_3* was performed on the top of the dune. For the inversion, we assumed that the aquifer is homogeneous and therefore adopted a water content of 26% everywhere in the aquifer below the dune. Considering this assumption, the resulting MRS log shows very good agreement with the borehole and TDEM results. The data are insufficient to comment on a small amount of water detected by MRS within the actual dune, but as the MRS measurements are of good quality, we believe that a small quantity of water is present.

3.4. Permeability estimation using magnetic resonance measurements

In NMR logging, T_1 and T_2 relaxation times are important for analysing the hydrodynamic properties of geological formations. Although there is a difference between these two parameters, both are used in

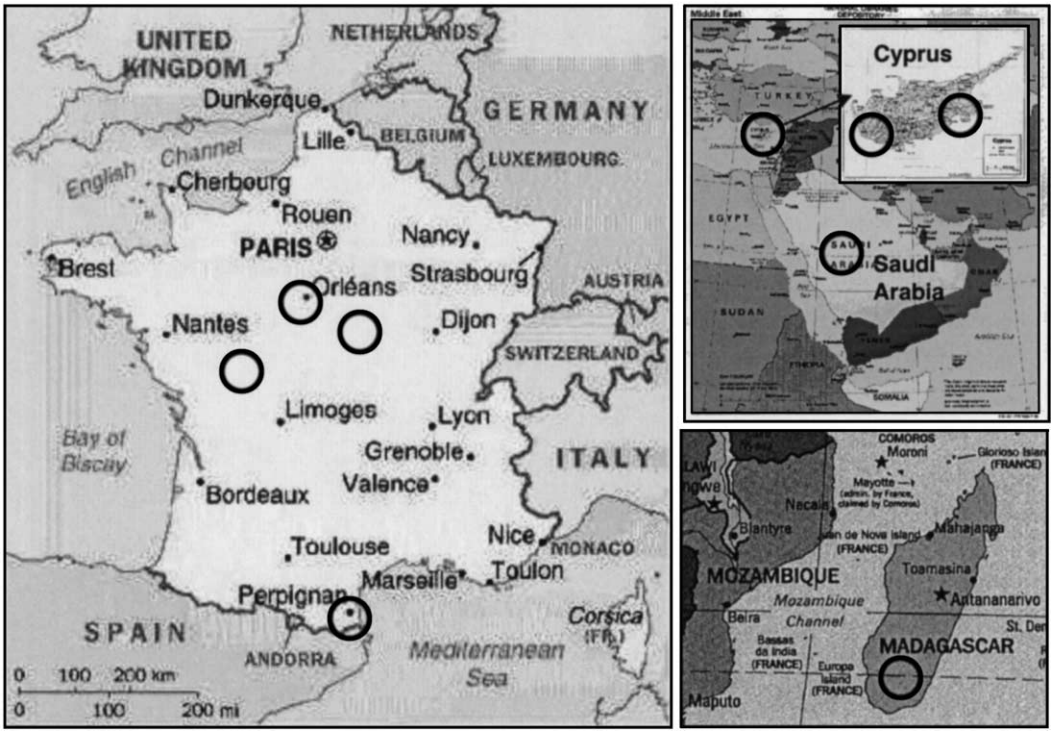

Fig. 13. Location of MRS test sites.

Table 1
Measurement of T_2^* and T_1 in various geological units

Rock type	Magnetization (A/m)	Susceptibility (SIU)	T_2^* (ms)	T_1 (ms)	Site	Comments
Reef limestone (bh3/99)	1.04×10^{-4}	-9.14×10^{-6}	80	220	Cyprus (Xilophagou)	Unsaturated zone above the static level
Fractured reef limestone (bh3/99)	2.81×10^{-4}	-8.45×10^{-6}	130	430	Cyprus (Xilophagou)	Saturated zone below the static level
Karst reef limestone	4.47×10^{-5}	-7.17×10^{-6}	460	1000	Cyprus (Xilophagou)	Saturated zone below the static level
Basaltic gravel	1.25×10^{-1}	4.80×10^{-3}	10	N/a	Cyprus (Phinicas)	Saturated zone below the static level
Sandstone	3.24×10^{-4}	1.99×10^{-4}	80	N/a	Cyprus (Xilophagou)	Saturated zone below the static level
Clay and fine sand	1.40×10^{-3}	1.35×10^{-4}	70	310	Mediterranean coast of France	Saturated zone below the static level
Medium sand	3.90×10^{-4}	2.91×10^{-5}	120	420	Mediterranean coast of France	Saturated zone below the static level
Highly fractured limestone	8.11×10^{-3}	1.48×10^{-3}	280	800	France (Villaimblain)	Saturated zone below the static level
Gravel and coarse sand	7.53×10^{-4}	4.39×10^{-4}	330	600	France (St-Cyr-en-Val)	Saturated zone below the static level

the analysis, and typically $T_1 \approx 1.5T_2$. T_1 and T_2 are related to pore size by

$$T_{1(2)} \sim V_p/S_p, \quad (5)$$

where V_p and S_p are the volume and surface area of the pore, respectively (Kenyon, 1997).

A specific study has been carried out in different geological environments (Fig. 13) using the NUMIS MRS equipment. The aim was to explore the possibility of expanding the experience gained through NMR logging to the surface application of magnetic resonance for the characterization of hydrodynamic properties of aquifers.

3.5. Relaxation time T_2^*

T_2^* relaxation time is usually used in MRS for the estimation of mean pore size: it varies from less than

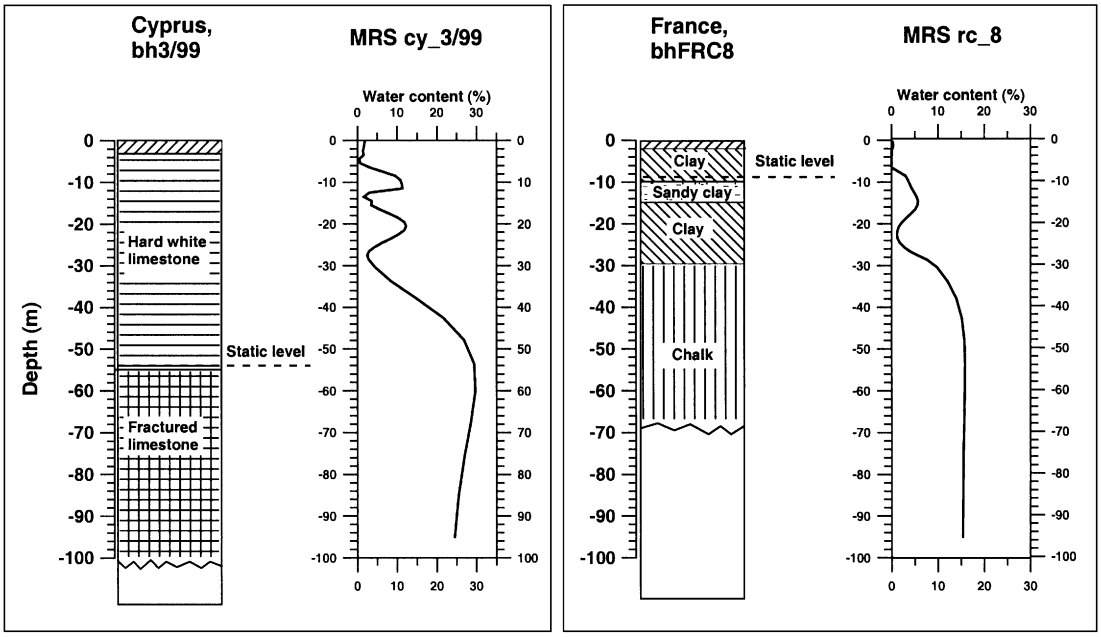

Fig. 14. Water distribution derived from MRS measurements in different geological formations.

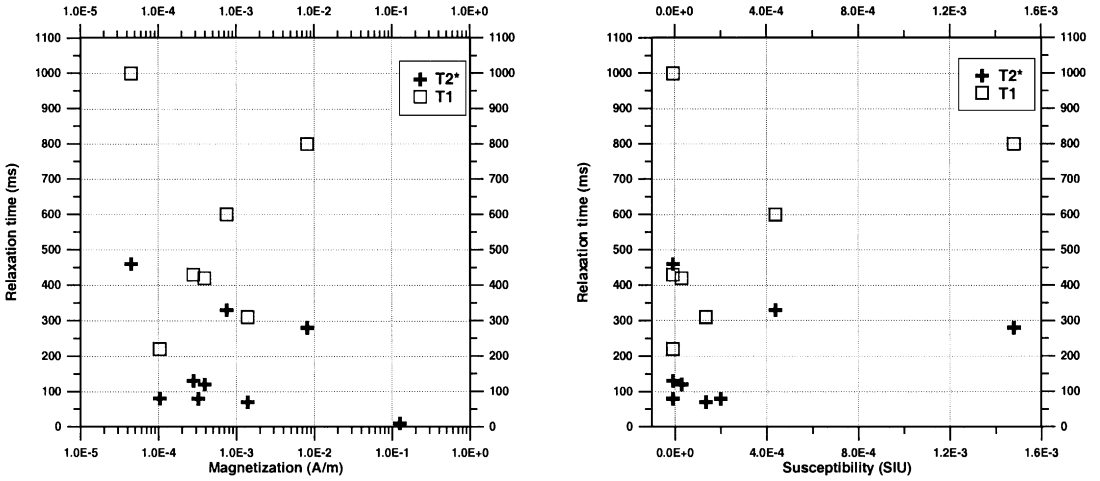

Fig. 15. Relaxation characteristics of the magnetic resonance signal measured in rocks with different magnetic properties.

30 ms in clay to 400–600 ms in gravel formation (Schirov et al., 1991). However, T_2^* is sensitive to local inhomogeneities in the geomagnetic field caused by variations in the magnetic properties of rocks, and hence should be less reliable than T_1 and T_2.

The results of T_1 and T_2^* measurement in aquifers composed of rocks with different magnetic properties (Table 1) show that the magnetization and magnetic susceptibility of rocks could completely disrupt the interpretation of MRS results. For example, MRS cannot generally detect short signals from bound water in the unsaturated zone. However, the magnetic resonance signal from the unsaturated zone was reliably measured in Cyprus as $T_2^* = 80$ ms because the reef limestone has a very low magnetic susceptibility ($M \approx 2 \times 10^{-4}$ A/m; $\chi = 8 \times 10^{-6}$ SIU). Another example is the basaltic gravel aquifer, also in Cyprus, that is highly magnetic ($M = 1.25 \times 10^{-1}$ A/m; $\chi = 4.8 \times 10^{-3}$ SIU). The yield of a borehole drilled here is about 100 m^3/h, but no signal was detected using the free induction decay method, which is currently the standard for MRS. Spin echo measurements carried out with a special set up of NUMIS equipment revealed that the signal is too short ($T_2^* = 10$ ms) for detection with the standard set up.

For demonstration purposes, we present the MRS results near two boreholes (Fig. 14), bh3/99 in Cyprus and bhFRC8 in France. In Cyprus, MRS detected some water in limestone below 5 m. Borehole measurements reveal the static level at 54 m and bound water in the limestone below 5 m. This confirms that for rocks with very low magnetic susceptibility, bound water in the unsaturated zone cannot be distinguished from water in the aquifer using MRS data alone. In France, the magnetic properties of the rocks are suitable for MRS ($M = 4 \times 10^{-4}$ A/m; $\chi = 1.5 \times 10^{-4}$ SIU), and two aquifers are well detected. These two examples clearly demonstrate that for a reliable interpretation, some calibration is necessary for the MRS response in the investigated geological formation.

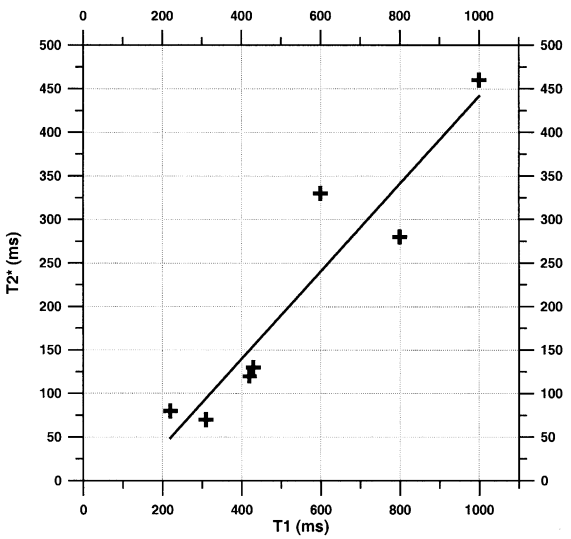

Fig. 16. Empirical relationship between T_1 and T_2^*.

In order to check whether in practice T_2^* is more sensitive to pore size or to the magnetic properties of rocks, values of T_1 (which depends essentially on pore size) and T_2^* measured in different rocks were plotted against the magnetization and susceptibility of these rocks (Fig. 15). The obtained results show that T_2^* is not strongly dependent on the magnetic properties of rocks. However, T_2^* plotted against T_1 (Fig. 16) reveals that on average, $T_1 = 2.2\ T_2^*$, which is in good agreement with the $T_1 \approx 1.5T_2$ estimation used in NMR logging and with the theoretical relationship $T_2^* < T_2 < T_1$. Our results are also in good agreement with other reported results of empirical estimations of pore size in aquifers using T_2^* measurements (Schirov et al., 1991; Leg-

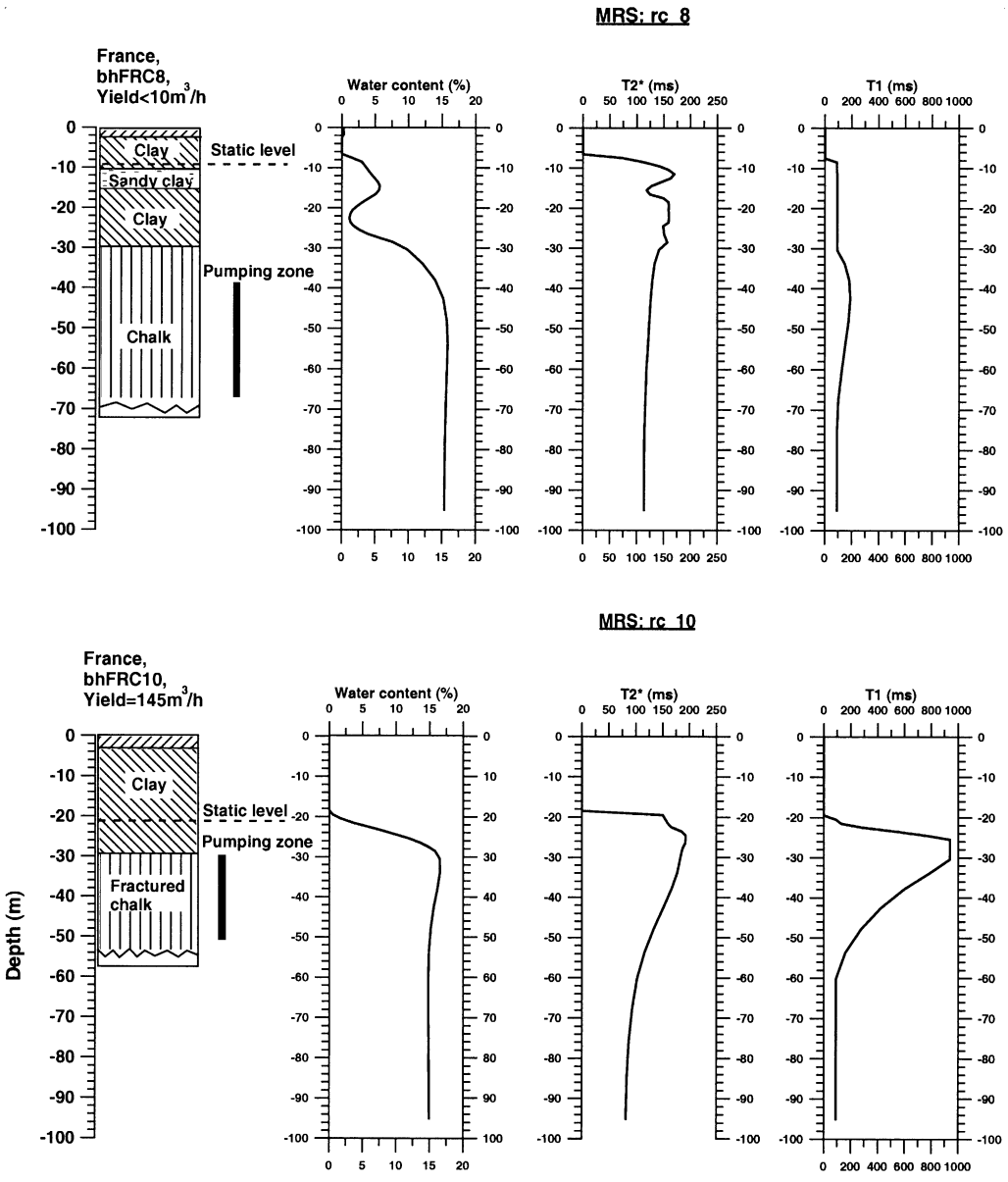

Fig. 17. Example of MRS results obtained near two boreholes with different yields.

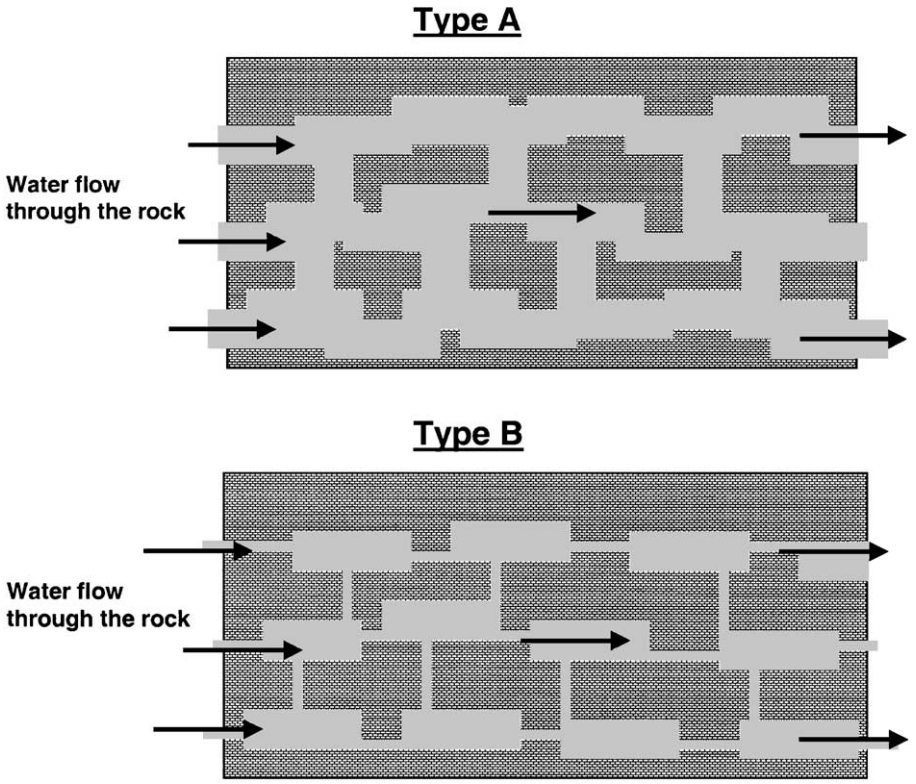

Fig. 18. The permeability of aquifers: type A—single porosity; type B—double porosity.

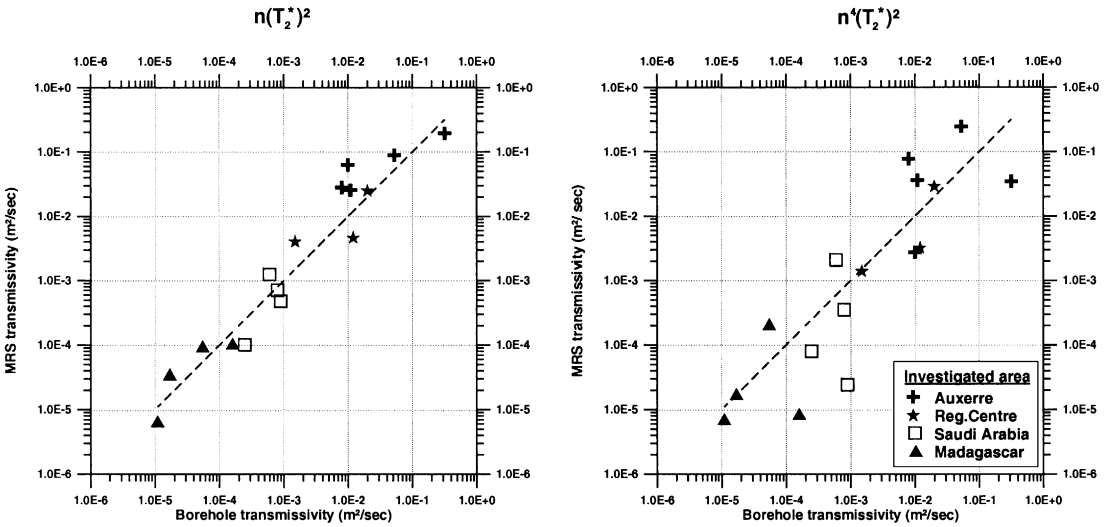

Fig. 19. Measured borehole transmissivity against estimated by MRS transmissivity using two different forms.

Table 2
Borehole data and MRS results

Area	Borehole	Rocks	T_{bh} (m^2/s)	Δz_{bh} (m)	MRS test site	w_{av} (%)	T^*_{2av} (ms)	T_{1av} (ms)	Δz_{MRS} (m)
France, Auxerre	St. Bris.	limestone	0.8×10^{-2}	10	ES3	20	60	Not available.	12
	P4	limestone	1.0×10^{-2}	9.6	ES5	5	180	N/a	12
	bh13	limestone	1.1×10^{-2}	10.7	ES2	16	70	N/a	10
	P1	limestone	5.3×10^{-2}	16.6	ES1	20	90	N/a	17
	P3	limestone	32×10^{-2}	11.1	ES6	8	250	N/a	12
France, Reg.Centre	bhFRC11	chalk	1.5×10^{-3}	10	RC11	7.2	144	332	9
	Lim/F1	limestone	1.2×10^{-2}	14	AvF1	9.1	130	797	10
	bhFRC10	chalk	2.0×10^{-2}	20	RC10	10.8	172	700	26
Saudi Arabia	bh16	diorite	2.5×10^{-4}	N/a	SA5	1.75	80	N/a	16
	bh5	diorite	6×10^{-4}	N/a	SA1	2.25	240	N/a	17
	bh14	diorite	8×10^{-4}	N/a	SA13	1.5	210	N/a	19
	bh14P2	diorite	9×10^{-4}	N/a	SA16	0.7	216	N/a	26
Madagascar	MD14	gneiss	1.1×10^{-5}	N/a	AND14	4.75	50	N/a	9
	MD2	gneiss	1.7×10^{-5}	N/a	AND2	3.65	150	N/a	7
	MD23	gneiss	5.5×10^{-5}	N/a	AND15	6	180	N/a	8
	MD5	gneiss	1.6×10^{-4}	N/a	AND6	2	175	N/a	28

Table 3
Empirical pre-factors for calculation of the transmissivity for different test sites

Area	$C^{T2*}_{p_1}$	$C^{T2*}_{p_2}$	$C^{T1}_{p_1}$	$C^{T1}_{p_2}$	Aquifer
Auxerre	3.26×10^{-8}	1.13×10^{-11}	N/a	N/a	Limestone
Region Centre	2.99×10^{-9}	2.76×10^{-12}	1.65×10^{-10}	1.53×10^{-13}	Limestone, sand, clay
Saudi Arabia	5.68×10^{-10}	8.34×10^{-11}	N/a	N/a	Fractured diorite
Madagascar	6.15×10^{-11}	6.25×10^{-13}	N/a	N/a	Fractured gneiss

chenko et al., 1997a; Yaramanci et al., 1999). For demonstration purposes, we present the MRS results obtained near two boreholes in France (Fig. 17). Since these two test sites are only about 2 km apart, a major difference is not expected in the magnetic properties of the subsurface. Although the water content was found

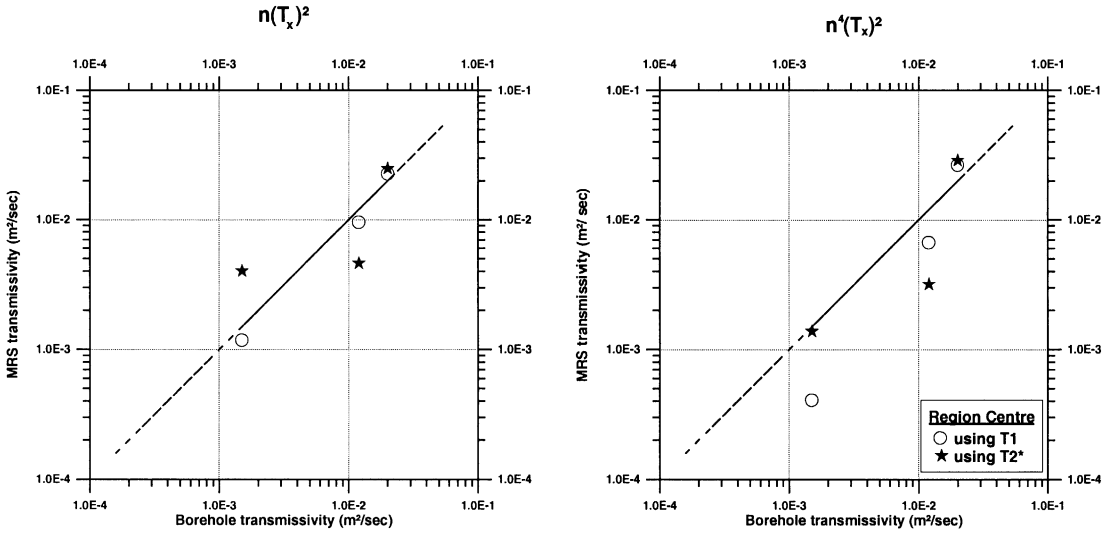

Fig. 20. Transmissivity estimation using T_1 and T^*_2.

to be very similar, this does not make it possible to distinguish which borehole has the higher yield, but the longer relaxation times measured at the MRS site *rc_10* correlate well with the higher yield of borehole bhFRC10.

3.6. Scale effect

The permeability of geological formations is scale-dependent. Since the samples investigated during laboratory, borehole NMR, and MRS experiments vary considerably in scale (Fig. 2), the results obtained with one method cannot be immediately extended to another. An example of two different types of aquifer is presented in Fig. 18. In aquifers with single porosity (type A), the water is located in similar pores and permeability is thus related to pore size. In this case, information concerning the aquifer derived from magnetic resonance measurements is also related to permeability, even when the investigated samples are of different volumes.

In aquifers with double porosity (type B), however, most of the water is located in large pores, but permeability mostly depends on small pores. In this case, when the volume of investigated sample is small, permeability estimation will depend on whether the selected sample mainly represents small or large pores. A large-scale method such as MRS will provide information mostly related to large pores because they contain a larger quantity of water than small pores.

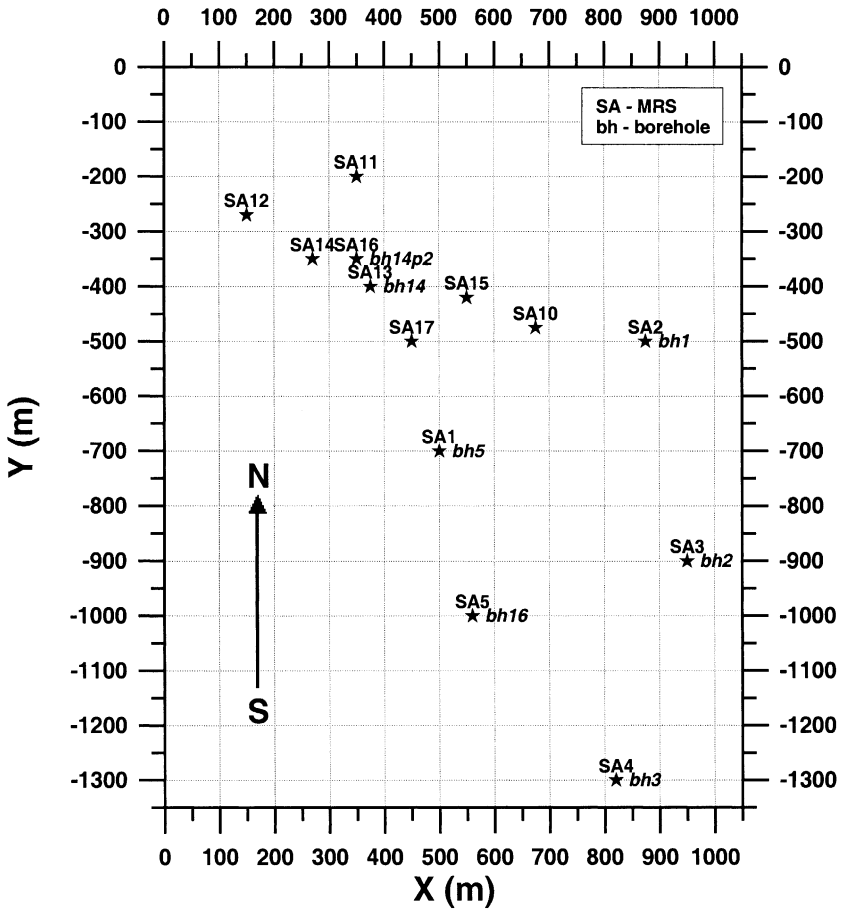

Fig. 21. Investigation grid in Saudi Arabia.

Table 4
MRS results for Saudi Arabia

MRS test site	X (m)	Y (m)	w_{av} (%)	T^*_{2av} (ms)	Δz_{MPS} (m)	MRS free water volume (m^3/m^2)	MRS specific yield ($m^3/h/m$)	MRS transmissivity (m^2/s)
SA1	500	−700	2.25	240	17	38.25	9.4	1.25×10^{-3}
SA2	875	−500	1.9	105	5	9.5	0.45	5.95×10^{-5}
SA3	950	−900	0.7	130	28	19.6	1.4	1.88×10^{-4}
SA4	820	−1300	1.25	135	14	17.5	1.36	1.81×10^{-4}
SA5	560	−1000	1.75	80	16	28	0.76	1.02×10^{-4}
SA10	675	−475	0.5	111	35	17.5	0.9	1.22×10^{-4}
SA11	350	−200	0.6	208	34	20.4	3.76	5.01×10^{-4}
SA12	150	−270	0.25	60	42	10.5	0.16	2.15×10^{-5}
SA13	375	−400	1.5	210	19	28.5	5.35	7.14×10^{-4}
SA14	270	−350	0.3	90	40	12	0.4	5.52×10^{-5}
SA15	550	−420	1	130	15	15	1.1	1.44×10^{-4}
SA16	350	−350	0.7	216	26	18.2	3.62	4.82×10^{-4}
SA17	450	−500	1.5	206	17	25.5	4.6	6.15×10^{-4}

Since large pores do not have a major influence on the permeability of the aquifer, the MRS estimation of the permeability might be erroneous.

These two extreme cases demonstrate the limitations of permeability estimation based on magnetic resonance measurements. In practice, different types of porosity usually co-exist, and the measured magnetic resonance signal is commonly multi-exponential and thus provides information concerning different pores.

3.7. MRS permeability estimation

Since geological formations with the same mean pore size estimated by magnetic resonance may have very different permeability, the estimation of permeability is more reliable when borehole pumping test results are available for calibration of the MRS data.

In NMR logging, permeability estimation is based on the form (Kenyon, 1997)

$$k = C_p \varphi^a_{NMR} T^b_{1(2)}, \quad (6)$$

where φ_{NMR} is the porosity estimated by NMR, $T_{1(2)}$ is T_1 or T_2 relaxation time, and C_p is an empirical prefactor. In our study, we compare the estimation form with $a=1$; $b=2$ introduced by Seevers (1966), and the estimator with $a=4$; $b=2$ that reportedly gives better results for sandstones (Kenyon et al., 1988). We also replace $T_{1(2)}$ by T^*_2 provided by NUMIS equipment.

Since both pumping tests and MRS are large-scale methods, an integral parameter is best suited to estimating the hydrodynamic parameters of aquifers. We use transmissivity $T=k\Delta z$, where k and Δz are aquifer permeability and thickness, respectively. Thus,

Table 5
Boreholes results for Saudi Arabia

Borehole	X (m)	Y (m)	Transmissivity (m^2/s)	Yield (m^3/h)	Drawdown (m)	Specific yield ($m^3/h/m$)	Corresponding MRS test site
bh5	500	−700	6.00×10^{-4}	22	2.2	10.00	SA1
bh1	875	−500	N/a	3	29	0.10	SA2
bh2	950	−900	N/a	4.5	4	1.13	SA3
bh3	820	−1300	N/a	7.2	12	0.60	SA4
bh16	560	−1000	2.50×10^{-4}	9.7	4.8	2.02	SA5
bh14	375	−400	8.00×10^{-4}	22	4.5	4.89	SA13
bh14p2	350	−350	9.00×10^{-4}	N/a	N/a	N/a	SA16

based on the MRS results, transmissivity is estimated as

$$T_{\mathrm{pmr1}} = C_{\mathrm{p_1}}^{T_2^*} \int_{\Delta z} w(T_2^*)^2 \mathrm{d}z, \tag{7}$$

and

$$T_{\mathrm{pmr2}} = C_{\mathrm{p_2}}^{T_2^*} \int_{\Delta z} w^4 (T_2^*)^2 \mathrm{d}z, \tag{8}$$

where $C_{\mathrm{p_1}}^{T2^*}$ and $C_{\mathrm{p_2}}^{T2^*}$ are the empirical pre-factors. If N boreholes are available for calibration in an investigated area, the empirical pre-factors can be calculated as

$$C_{\mathrm{p}} = \frac{\sum_{i=1}^{N} T_{i\_\mathrm{bh}}}{\sum_{i=1}^{N} F_i}, \tag{9}$$

where T_{i_bh} is the transmissivity given by a pumping test in borehole i, and $F_i = \int_{\Delta z} w^a (T_2^*)^b \mathrm{d}z$ is the MRS estimation form.

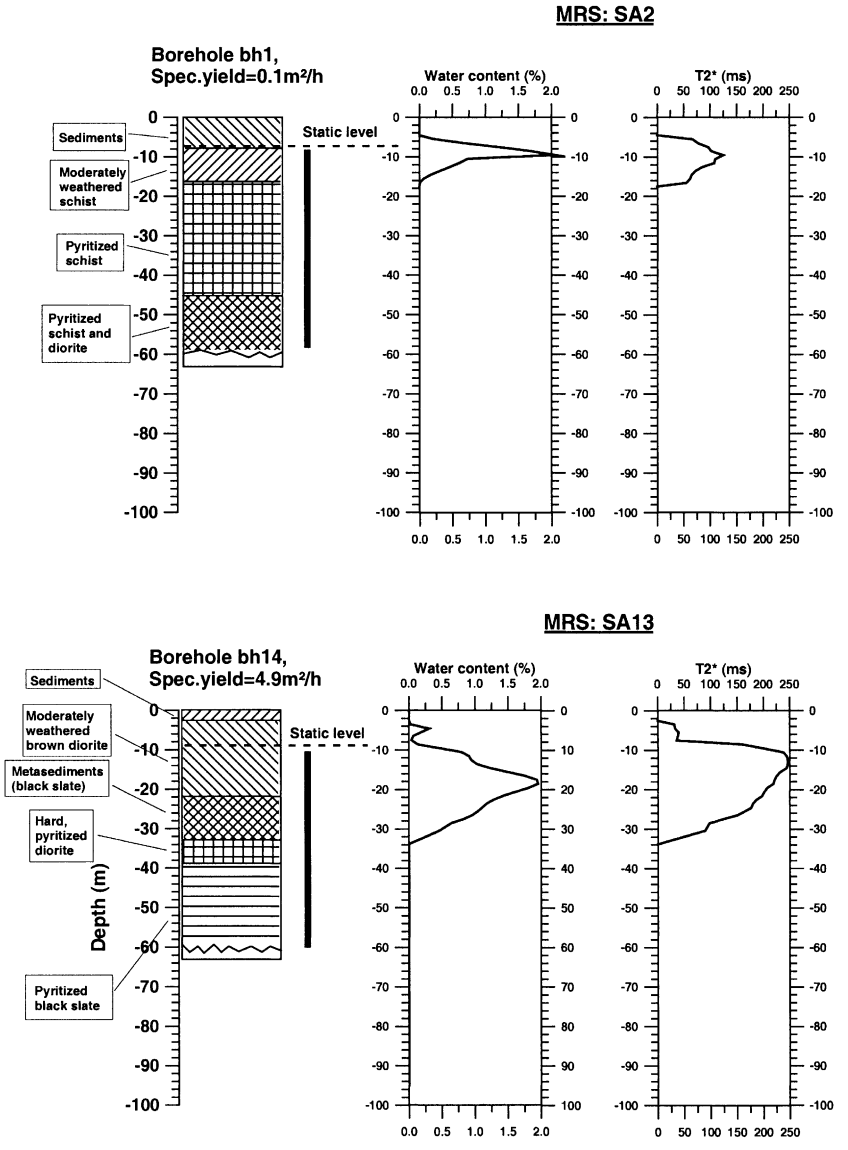

Fig. 22. Example of MRS results obtained in Saudi Arabia near two boreholes with different yields.

When T_1 relaxation time measurements are available, T_1 can replace T_2^* in Eqs. (7) and (8), and the empirical pre-factor ($C_{p_1}^{T1}$ or $C_{p_2}^{T1}$) should also be calculated using T_1 values in Eq. (9).

The results of transmissivity estimated from MRS and transmissivity measured during borehole pumping tests are presented in Fig. 19 and Table 2. Since in different areas the test sites are made up of different geological formations, empirical pre-factors were calculated separately for each area (Table 3). A large difference in the pre-factor values experimentally observed confirms the need for calibration. A better correspondence was observed between borehole data and MRS estimation when the $a=1$; $b=2$ form proposed by Seevers (1966) was adopted. As we have not enough data to be able to establish reliable empirical relationship between hydrodynamic properties of aquifers and MRS results for different geological formations, we consider our results as a preliminary demonstration for this possibility.

A few results where T_1 relaxation times were available seem promising (Fig. 20), which confirms a theoretical expectation. However, because T_1 measurement requires a double pulse and is more time consuming, more data are needed for a definitive conclusion.

3.8. Example of an MRS survey

An MRS survey was carried out in Saudi Arabia (Legchenko et al., 1998). The aquifer in investigated area is composed of fractured diorite. The pumping tests were carried out using the total interval from the water table down to about 60 m what do not allow us to identify the exact geometry of this rather heterogeneous aquifer. We also have no information about hydrogeological modeling in this area. Taking into account the complexity of the aquifer and insufficient hydrogeological data available we consider presented example as just a demonstration of the MRS potential.

The test site locations within the investigation grid are presented in Fig. 21. Since specific yield is also commonly used for estimating the hydrodynamic properties of aquifers, both transmissivity and specific yield were estimated from the MRS data using estimators given by Eq. (7) and calibration wells. The MRS results are summarized in Table 4. Data from seven boreholes (Table 5) were used for calibration of and comparison with the MRS data.

Two borehole sections and the results from their corresponding MRS sites are depicted in Fig. 22. In both cases, the static level detected by MRS and that measured in the boreholes show good agreement. Although the water content was found to be about 2% at both sites, the MRS results reveal a greater thickness and a longer relaxation time T_2^* for sounding *SA_13*, which corresponds to the higher specific yield of borehole *bh14*. The results of specific yield estimated from MRS versus specific yield measured in boreholes (Fig. 23) are generally in good agreement.

Following the water content definition (Eq. (4)), for each sounding we can estimate a free water volume per square meter as

$$V_{\mathrm{pmr}} = C_{\mathrm{W}} \int_z w(z)\mathrm{d}z. \tag{10}$$

As a laboratory calibration for the water content was not available, we assumed $C_{\mathrm{W}}=1$ and drew up a relative map of free water distribution (Fig. 24), which

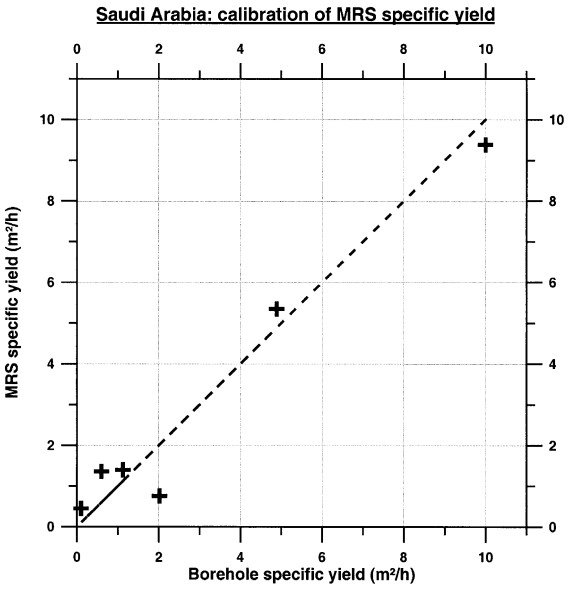

Fig. 23. Estimated MRS specific yield versus measured borehole specific yield in Saudi Arabia.

enables the location of water-storage zones in the investigated area.

A map of estimated MRS transmissivity is presented in Fig. 25. The maps of specific yield estimated from MRS and specific yield measured during borehole pumping tests (Fig. 26) show a good correlation.

In summary, all the results obtained through MRS are in good agreement and correlate well with the borehole results. On this basis, we can propose the application of the MRS method for aquifer characterization in hard-rock environments. The MRS method could be used in conjunction with hydrogeological modeling for better definition of boundary conditions and for the location of water-storage areas.

Our first experience shows that the MRS can be also applied to estimation of hydrodynamic properties of aquifers. However, the development of an effective and reliable methodology of MRS application in different geological conditions needs further research efforts.

4. Conclusions

The proton Magnetic Resonance Sounding method is a geophysical tool that provides information concerning groundwater distribution in the subsurface. While other geophysical methods are able to detect inhomogeneities in the physical properties of rocks,

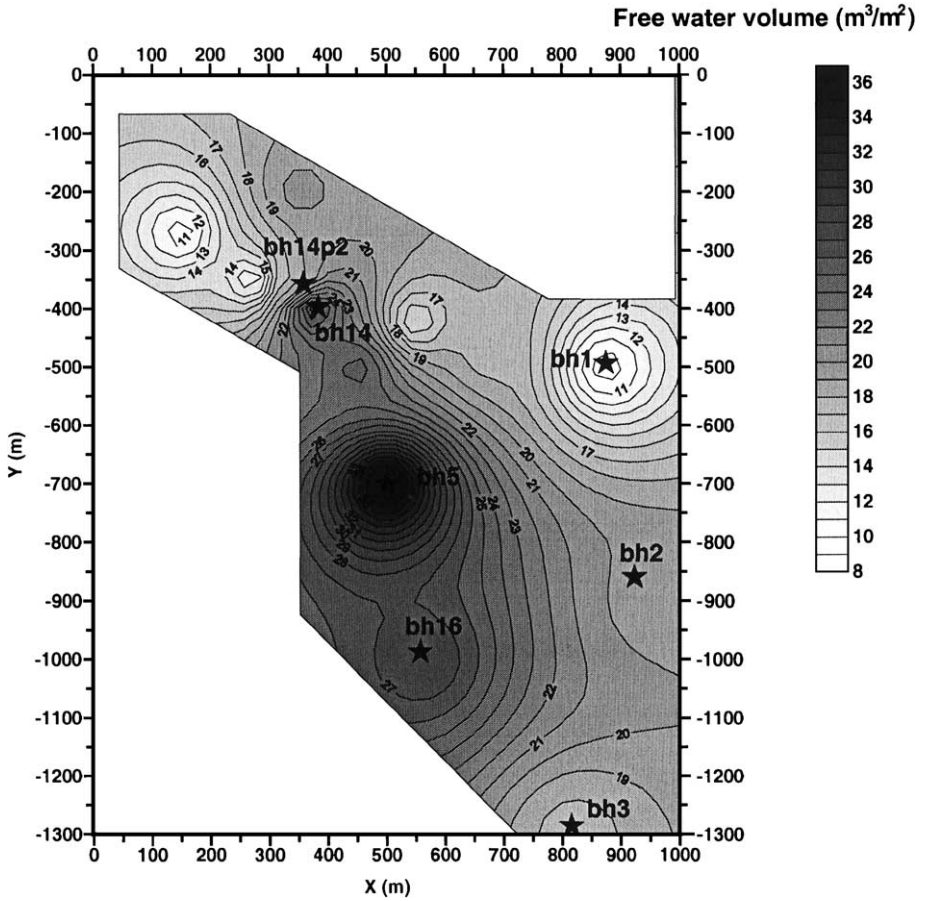

Fig. 24. Map of MRS free water distribution in Saudi Arabia.

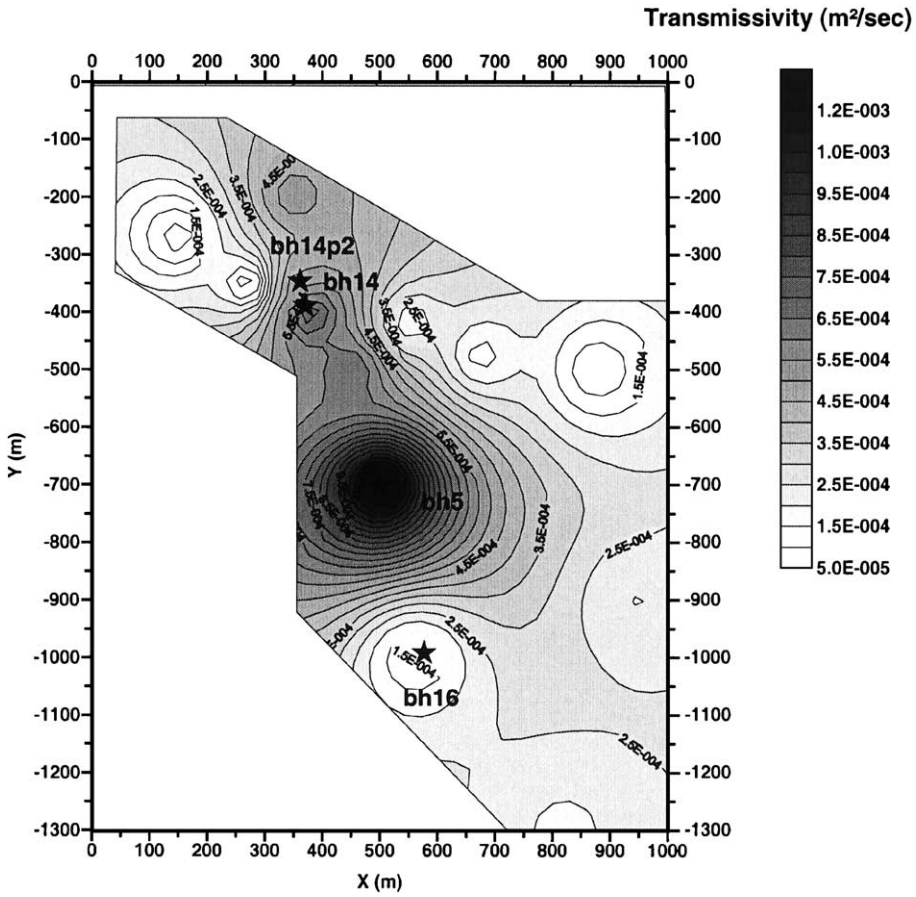

Fig. 25. Map of estimated MRS transmissivity in Saudi Arabia.

the magnetic resonance signal that is generated by groundwater molecules can be used for the estimation of the quantity of water in the subsurface and of the hydrodynamic characteristics of aquifers.

MRS is a site-dependent method. The geomagnetic field and the electrical conductivity of the subsurface are major factors that influence the performance of the method. For example, where the resistivity of the subsurface is larger than 50 Ω m, groundwater can be detected down to more than 150 m in areas with a high geomagnetic field and only down to about 100 m in areas with a low geomagnetic field. Electrically conductive rocks attenuate the magnetic resonance signal and thus diminish the maximum depth of investigation down to 40–50 m.

The water content and the relaxation times T_1 and T_2^* measured by MRS equipment can be used to estimate permeability, transmissivity and specific yield when calibration is possible using data from a borehole drilled in the same formation. The best form for permeability estimation was found to be $k \sim wT_x^2$, where w is water content and T_x is T_1 or T_2^* relaxation time. Since T_2^* is sensitive to the magnetic properties of rocks, T_1 should be a more reliable parameter. Preliminary results confirm this theoretical expectation, but as T_1 measurement is more time and energy consuming, we do not have sufficient experience as yet to draw a definitive conclusion.

MRS is a large-scale method. Since it provides results averaged over the entire loop area, it may not

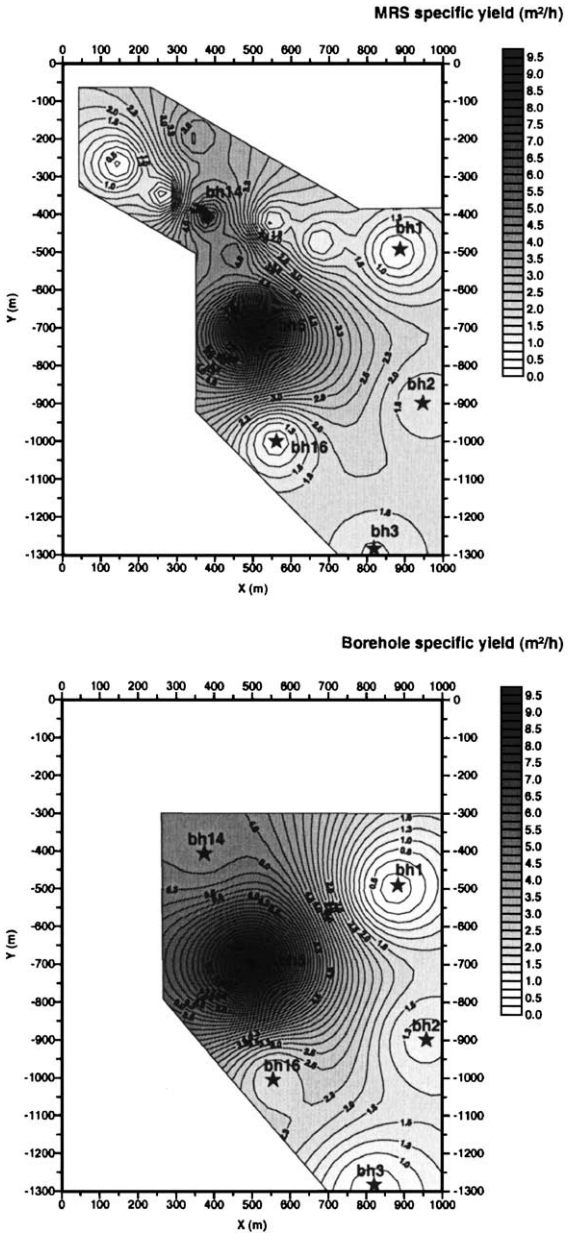

Fig. 26. Maps of estimated MRS specific yield and measured borehole specific yield in Saudi Arabia.

be sufficiently accurate for detecting small targets (for example a single fracture). It is, however, effective for estimating water resources and for mapping the average hydrodynamic properties of an investigated area when some calibration with boreholes is possible.

Acknowledgements

The authors would like to acknowledge the assistance of Gilles Grandjean of BRGM for his participation in the fieldwork and Yves Albouy of IRD for providing us with the TDEM data in the Dune du Pilat area. We also thank Pierre Valla of IRIS Instruments and Patrick Lachassagne of BRGM for fruitful discussions and Rowena Stead of BRGM for language corrections. The presented results were obtained in the framework of the BRGM research project PRD319 and the European Project INCO-DC No. CT960122.

References

Gev, I., Goldman, M., Rabinovich, B., Rabinovich, M., Issar, A., 1996. Detection of the level in fractured phreatic aquifers using nuclear magnetic resonance (NMR) geophysical measurements. J. Appl. Geophys. 34, 277–282.

Goldman, M., Rabinovich, B., Rabinovich, M., Gilad, D., Gev, I., Schirov, M., 1994. Application of integrated NMR-TDEM method in ground water exploration in Israel. J. Appl. Geophys. 31, 27–52.

Guillen, A., Legchenko, A.V., 1997. Inverse problem of magnetic resonance measurements applied to water resource characterization. Expanded Abstracts, SEG'97, Dallas (USA), November 2–7, vol. I, pp. 446–449.

Guillen, A., Legchenko, A.V., 1998. Inversion of 1D NMR data by the Monte-Carlo Method. Proceedings, NMR Imaging of Reservoir Attributes, SEG Summer research Workshop, August 9–12, 1998, Park City, UT, USA.

Kenyon, W.E., 1997. Petrophysical principles of applications of NMR logging. Log Anal., pp. 21–43, March–April.

Kenyon, W.E., Day, P.I., Straley, C., Willemsen, J.F., 1988. A three-part study of NMR longitudinal relaxation properties of water-saturated sandstones. SPE Form. Eval. 3, 622–636.

Legchenko, A.V., Shushakov, O.A., 1998. Inversion of surface NMR data. Geophysics 63 (1), 75–84.

Legchenko, A.V., Shushakov, O.A., Perrin, J., Portselan, A.A., 1995. Noninvasive NMR study of subsurface aquifers in France. Abstracts of The International Exposition and SEG'95 Annual Meeting, October 9–12, 1995, Houston, USA, pp. 365–367.

Legchenko, A.V., Baltassat, J.-M., Beauce, A., Chigot, D., 1997a. Application of proton magnetic resonance for detection of fractured chalk aquifers from the surface. Proceedings of the 3rd Meeting on Environmental and Engineering Geophysics, Aarhus (Denmark), 8–11 Sept. 1997, pp. 115–118.

Legchenko, A.V., Beauce, A., Guillen, A., Valla, P., Bernard, J., 1997b. Natural variations in the magnetic resonance signal used in PMR groundwater prospecting from the surface. Eur. J. Environ. Eng. Geophys. 2, 173–190.

Legchenko, A.V., Baltassat, J.M., Beauce, A., Makki, M.A., Al-Gaydi, B.A., 1998. Application of the surface proton magnetic reso-

nance method for the detection of fractured granite aquifers. Proceedings of the IV Meeting of the Environmental and Engineering Geophysical Society (European Section), September 14–17, 1998, Barcelona (Spain), pp. 163–166.

Lieblich, D.A., Legchenko, A., Haeni, F.P., Portselan, A., 1994. Surface nuclear magnetic resonance experiments to detect subsurface water at Haddam Meadows, Connecticut. Proceedings of the Symposium on the Application of Geophysics to Engineering and Environmental Problems, March 27–31, 1994, Boston, MA, vol. 2, pp. 717–736.

Schirov, M., Legchenko, A., Creer, G., 1991. New direct non-invasive ground water detection technology for Australia. Explor. Geophys. 22, 333–338.

Semenov, A.G., 1987. NMR Hydroscope for water prospecting. Proceedings of the Seminar on Geotomography, Indian Geophysical Union, Hyderabad, pp. 66–67.

Semenov, A.G., Schirov, M.D., Legchenko, A.V., 1987. On the technology of subterranean water exploration founded on application of nuclear magnetic resonance tomograph Hydroscope. IXth Ampere summer school, Abstracts, Novosibirsk, September 20–26, p. 214.

Semenov, A.G., Burshtein, A.I., Pusep, A.Yu., Schirov, M.D., 1988. A device for measurement of underground mineral parameters, USSR Patent 1079063 (in Russian).

Seevers, D.O., 1966. A nuclear magnetic method for determining the permeability of sandstones, paper L. Annual Logging Symposium Transactions: Society of Professional Well Log Analysts.

Shushakov, O.A., 1996. Groundwater NMR in conductive water. Geophysics 61 (4), 998–1006.

Slichter, C.P., 1990. Principles of Magnetic Resonance, 3rd edn. Springer-Verlag, Berlin, 655 pp.

Varian, R.H., 1962, Ground liquid prospecting method and apparatus, US Patent 3019383.

Yaramanci, U., Lange, G., Nodel, K., 1999. Surface NMR within a geophysical study of an aquifer at Haldensleben (Germany). Geophys. Prospect. 47, 923–943.